RSC Advances

PAPER

View Article Online
View Journal | View Issue

Cite this: *RSC Adv.*, 2022, **12**, 17257

The effect of heteroatom doping on the active metal site of CoS_2 for hydrogen evolution reaction

Jianjian Shi, [a] Tao Chen*[a] and Xiaoli Sun*[bc]

The exploration of cost-effective hydrogen evolution reaction (HER) electrocatalysts through water splitting is important for developing clean energy technology and devices. The application of CoS_2 in HER has been drawing more and more attention due to its low cost and relatively satisfactory HER catalytic performance. And CoS_2 was found to exhibit excellent HER catalytic performance after appropriate doping according to other experimental investigations. However, the theoretical simulation and the intrinsic catalytic mechanism of CoS_2 remains insufficiently investigated. Therefore, in this study, density functional theory is used to investigate the HER catalytic activity of CoS_2 doped with a heteroatom. The results show that Pt-, N- and O-doped CoS_2 demonstrates smaller Gibbs free energies close to that of Pt, compared with the original CoS_2 and CoS_2 doped with other atoms. Furthermore, HER catalytic performance of CoS_2 can be improved by tuning d-band centers of H adsorption sites. This study provides an effective method to achieve modified CoS_2 for high-performance HER and to investigate other transition metal sulfides as HER electrode.

Received 23rd March 2022
Accepted 1st June 2022

DOI: 10.1039/d2ra01865a

rsc.li/rsc-advances

1 Introduction

The high combustion heat value, clean combustion products, and abundant resources make hydrogen (H_2) a distinguished energy storage material. Producing hydrogen from the electrochemical decomposition of water (H_2O), the commonly believed future energy carrier,[1,2] through hydrogen evolution reaction (HER) has been proved to be a clean and renewable method. However, the hydrogen production catalyst precious metal platinum (Pt), the most efficient electrocatalyst for HER owing to its high stability, low overpotential (about 0.08 V), as well low Tafel slope,[3] has not been applied on large scales due to its high cost and scarcity. Hence, it is quite necessary to find a new high-performance HER catalyst.

In recent decades, transition metal sulfides (TMSs), such as MoS_2,[4–10] VS_2,[11–15] CoS_2,[2,16–20] NiS_2 (ref. 2, 7, 15, 21 and 22) have been attracting attention from researchers and industry practitioners. Though the effects of the aforesaid compounds as hydrogen production catalysts had been considered in some previous studies, the more recent ones show that some of them such as HER electrode material can exhibit outstanding electrocatalytic performance that is close to that of precious metals (such as Pt). To further optimize the performance of the TMSs, some other studies suggest the incorporating of a third heteroatom in a binary compound, which can improve the electrocatalytic activity of the catalyst.[23]

As a representative of pyrite-type transition metal sulfides, CoS_2 is a low-cost catalytic material with excellent HER performance. Unfortunately, when doping CoS_2 with a third heteroatom, no good descriptor can be found to describe the relationship between the structure and activity of the doped CoS_2, and the inherent mechanism remains insufficiently explored.

It is noteworthy that Hoffmann *et al.* found that the center of the d-band formed by the TM turned out to be a good descriptor to predict the adsorption and reactivity of transition metal catalysts.[24] Furthermore, an analogous model of d-band based on surface resonance states has also been developed in the transition metal carbides (TMCs),[25] metal nitrides (MNs),[26] and layered TMSs.[27] This can significantly contribute to the analysis of structure–activity relationships in TMCs/TMSs, which can further help improve the design and high-throughput screening of catalysts. Many studies have also found that doping can change the energy band structure near the Fermi energy, so as to change the properties of materials.[10,28,29] Therefore, we take interest in investigating the possibility to doped CoS_2 for high-performance HER by tuning the d-band centers.

In this work, we study the effect of a heteroatom doping on HER electrochemical properties for CoS_2 electrode material based on density functional theory and explore the structure–activity relationships. Herein, the models of the pristine CoS_2 and doped CoS_2 were built, the stability, the catalytic activity, and the d-band centers of the active metal sites of CoS_2 doped with a heteroatom (Mn, Fe, Ni, Cu, Mo, Pt, Ru, C, N, O, P) are

[a]*School of Electronic Engineering, Chengdu Technological University, Chengdu 611730, PR China. E-mail: sjjian@cdtu.edu.cn; 570560423@qq.com*

[b]*Department of Energy and Power Engineering, Tsinghua University, Beijing, 100084, P. R. China. E-mail: sunxiaolideyuye@163.com*

[c]*Beijing Graphene Institute, Beijing 100095, P. R. China*

studied based on density functional theory (DFT). Our first-principles calculations exhibit that the structures of all doped CoS_2 except C-doped CoS_2 are stable, the catalytic behavior of CoS_2 can be effectively enhanced after Pt, N, and O doping, and the HER catalysis of CoS_2 can be changed by tailoring the d-band centers of active metal sites. Our studies are of great benefit to uncovering the intrinsic modulation mechanism of CoS_2 for HER catalysis.

2 Computational methods

All density functional theory (DFT) simulations were employed using the Generalized Gradient Approximation-Perdew Burke Ernzerhof (GGA-PBE) was used for the exchange-correlation term in the Spanish Initiative for Electronic Simulations with Thousands of Atoms (SIESTA).[30,31] The geometric optimization was employed using a conjugate gradient method until the maximum force was less than 0.02 eV $Å^{-1}$. An energy cut-off for all simulations was set to be 150 Ry.

2.1 Bulk CoS_2

The *k*-point mesh is set as Γ-centered 7 × 7 × 7 to relax the CoS_2 unit cell with a space group of $Pa\bar{3}$. The calculated CoS_2 unit cell parameter is 5.544 Å, which is highly consistent with the experimental value (5.538 Å).[23,32] The optimized bulk structure is shown in Fig. 1, where the big and small balls represent Co and S atoms, respectively.

2.2 CoS_2(001) surface

The (001) surface of CoS_2 is selected as the optimization model owing to its stability,[32] which is built as a 2 × 2 repeating surface unit cells consisting of four S–Co–S atomic layers and 8 CoS_2 units. Cation-doped CoS_2 is acquired by replacing one Co atom with one metal atom, and anion-doped CoS_2 is acquired by replacing one S atom with one nonmetal atom. A vacuum layer with a thickness of 15 Å is introduced to reduce interaction between periodic images.[33] The CoS_2(001) crystalline structure is represented in Fig. 2.

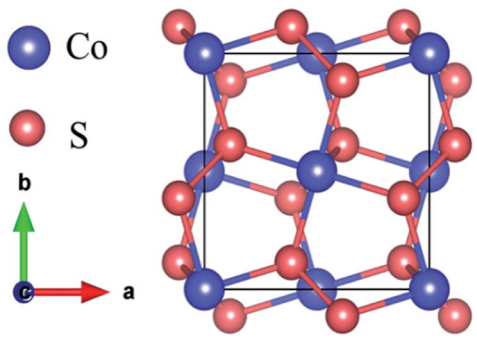

Fig. 1 The optimized structure of the bulk CoS_2.

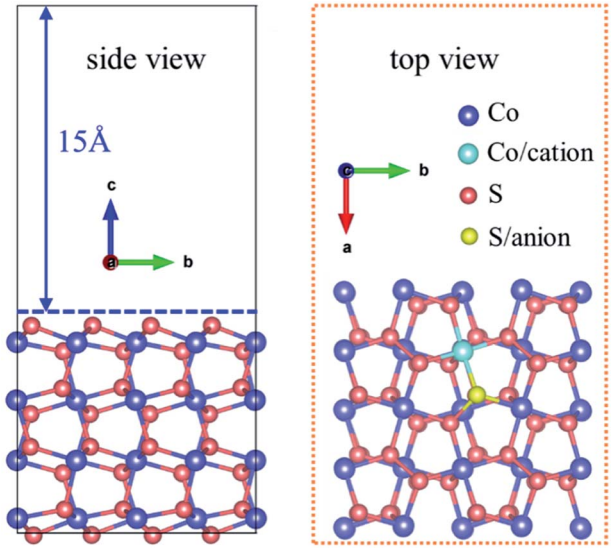

Fig. 2 The crystallographic structure of CoS_2(001) surface.

2.3 Binding energy

The binding energies (E_b) were first calculated to measure the stability of CoS_2 after doping, E_b is the difference between the cohesive energy (E_{coh}) of cubic CoS_2 and the embedding energy of the dopants (E_{emb}) on the CoS_2 surface.[34]

$$E_{coh} = E_{bulk} - E_{iso} \quad (1)$$

$$E_{emb} = E_{dopant+subs} - E_{subs} - E_{iso} \quad (2)$$

$$E_b = E_{coh} - E_{emb} \quad (3)$$

where E_{bulk} is the total energy of an atom in the bulk, E_{iso} is the total energy of an isolated atom, $E_{dopants+subs}$ is the total energy of doped CoS_2, and E_{subs} is the total energy of CoS_2 with one vacancy.

2.4 Gibbs free energy of H adsorption

Nørskov *et al.*[3] showed that with the absolute Gibbs free energy of hydrogen adsorption (ΔG_{H^*}) approximating zero, the binding between HER intermediates and the electrode surface was neither too strong nor too weak, demonstrating a high catalytic performance of HER. Hence, the (ΔG_{H^*}) as a significant factor of measuring the HER catalytic activity is quite essential to is calculated using reliable DFT simulations.[35] In our work, the HER catalytic properties in acidic media were investigated. While considering the HER reaction process in acid, the Volmer reaction[3] was selected under our calculations, because most reactions occur in protic solution or involve proton as the reactant:[36] $H^+(sol) + e^- \rightarrow H^*$, where H* refers to H adsorbed on the active site, and many studies analyze the electrochemical catalytic properties of HER based on the Volmer reaction.[3] The Gibbs free energy of hydrogen adsorption ((ΔG_{H^*})) as a significant factor of measuring the HER catalytic activity is calculated

Table 1 Binding energies of doped CoS_2 (E_b, eV)

Cation	Model	Mn	Fe	Ni	Cu	Mo	Pt	Ru
	E_b/eV	−2.89	−2.02	−1.67	−0.96	−1.78	−1.41	−1.97

Anion	Model	C	N	O	P
	E_b/eV	1.96	−1.67	−2.27	−1.52

based on the Volmer reaction using the DFT method. Its definition is as follows[35]

$$\Delta G_{H^*} = \Delta E_H + \Delta E_{ZPE} - T\Delta S \quad (4)$$

where ΔE_{ZPE} is the difference in zero-point energy between the adsorption state of H and gas phase, while ΔS is the difference in entropy between the adsorption state of H and gas phase.[3] ΔE_H is the hydrogen adsorption energy. Given that the vibrational entropy of H* in the adsorbed state is small, the entropy of adsorption of $-1/2H_2$ is simplified as $\Delta S_H \approx -1/2S_{H_2}{}^0$, where $S_{H_2}{}^0$ is the entropy of H_2 in the gas phase at standard conditions. Therefore, the overall corrections of ΔG_{H^*} are[3]

$$\Delta G_{H^*} = \Delta E_H + 0.24 \text{ eV} \quad (5)$$

The hydrogen adsorption energy (ΔE_H) on the electrode surfaces is defined as

$$\Delta E_H = E_{subs+H^*} - E_{subs} - \frac{1}{2}E_{H_2} \quad (6)$$

where E_{subs+H^*} is the total energy of doped $CoS_2(001)$ with H* adsorption, E_{subs} is the total energy of doped $CoS_2(001)$ without H* adsorption, and E_{H_2} is the total energy for one hydrogen molecule in the gas phase.

2.5 d-band centers

To further explore the possibility of enhancing electrochemical performance of CoS_2 *via* doping, we calculated the d-band center of the metal at active site.

The d-band center ε_d is defined as

$$\varepsilon_d = \frac{\int_{-\infty}^{\infty} \rho(\varepsilon)\varepsilon d\varepsilon}{\int_{-\infty}^{\infty} \rho(\varepsilon) d\varepsilon} \quad (7)$$

where ρ are the densities of states and ε are the energies.

3 Results and discussion

Some materials demonstrate good computational performance but are difficult to synthesize due to their aggregation- or clustering-related instability, which limits their application in experiments or in practice.[37] So, it is important to first investigate the stability of CoS_2 in order to explore the possibility of its synthesis. We use the binding energy (E_b) descriptor to measure the stability of doped CoS_2, if, $E_b < 0$, the atoms shows more tendency of being incorporated into the $CoS_2(001)$ surface rather than clustering or aggregation, and then we regard that the material satisfies the stability criterion.[34] The calculated binding energies are listed in Table 1. From Table 1 we can see, E_b of all cation and anion doped CoS_2 except for C-doped CoS_2 are less than zero, which demonstrates that it is energetically possible for one cation dopant to replace one Co atom in the $CoS_2(001)$ surface and for one anion dopant to replace one S atom in the $CoS_2(001)$ surface. However, the binding energy is

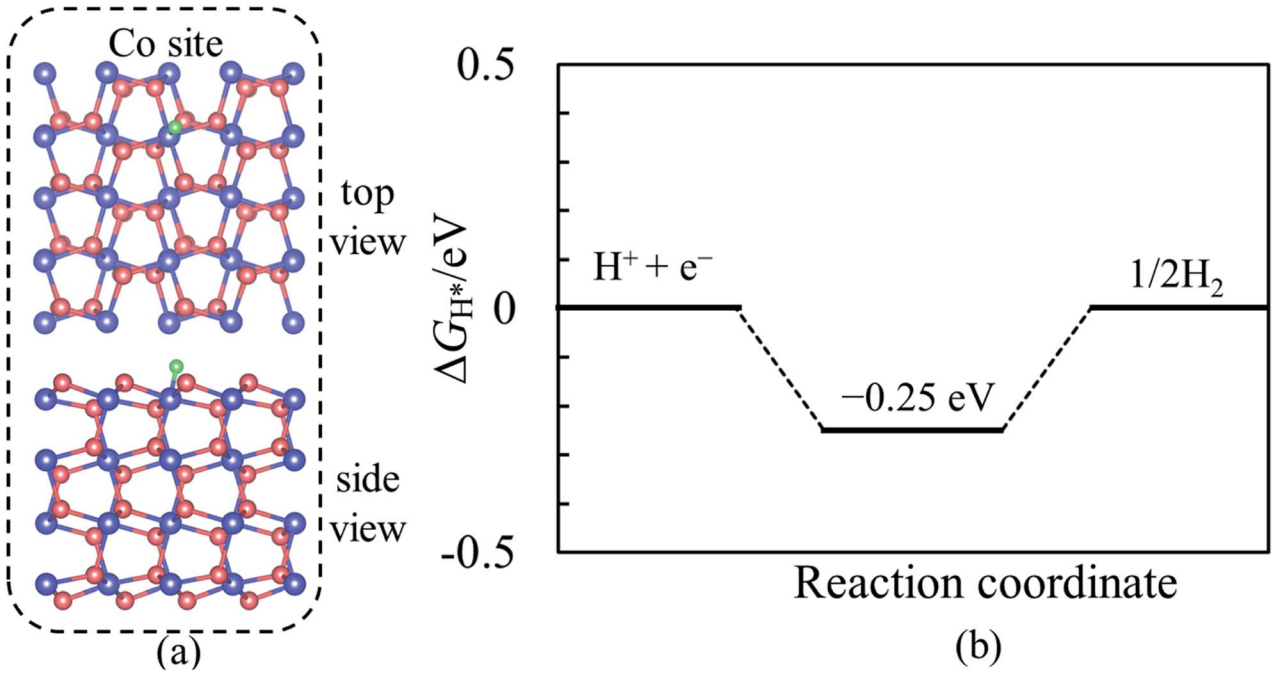

Fig. 3 (a) Represents the H adsorption structure of the pristine CoS_2, where H adsorbs at Co site. The green ball refers to H atom. (b) is ΔG_{H^*} diagram of the pristine CoS_2.

1.96 eV when one S atom in the $CoS_2(001)$ surface is substituted by one C atom, which is much higher than zero, indicating that when one C is incorporated into the $CoS_2(001)$, it tends to take the form of cluster or aggregation, which causes an unstable C-doped $CoS_2(001)$ structure. Therefore, C will not be considered as a heteroatom to form a HER catalyst.

After identifying the stability for a cation/anion heteroatom incorporated into the $CoS_2(001)$ surface, the state of the adsorbed H was discussed according to H adsorption energy. The negative value means that H is easy to bind to the $CoS_2(001)$.[38–40] The value of adsorption energy for 11 doped-CoS_2 are from −1.43 eV to −2.46 eV, which indicates that it is feasible to H bind to the surface of $CoS_2(001)$. Moreover, the catalytic performance for HER of the $CoS_2(001)$ with and without cation/anion heteroatom doping was investigated. To determine whether CoS_2 is an outstanding HER catalyst, the Gibbs free energies (ΔG_{H^*}) for hydrogen adsorption at active metal sites were calculated based on the DFT method. Fig. 3(a) is the relaxed crystallographic structure of H adsorption at the Co site for the pure $CoS_2(001)$, in which the green ball refers to H atom. The Co–H bond length is 1.50 Å. The calculated $|\Delta G_{H^*}|$ of the pure $CoS_2(001)$ is 0.25 eV, as shown in Fig. 3(b), which is larger than that of the precious metal Pt (0.08 eV).[3] In order to further probe the effect of heteroatom atoms on electrochemical HER catalytic performance for $CoS_2(001)$ as electrode material, the ΔG_{H^*} of cation- (Mn, Fe, Ni, Cu, Mo, Pt and Ru) and anion- (N, O and P) doped CoS_2 are calculated using the DFT method. Fig. 4(a) and (c) show the calculated ΔG_{H^*} of H adsorption at the active metal sites for cation- and anion-doped $CoS_2(001)$, respectively. In Fig. 4(a) and (c), ΔG_{H^*} of Ni-doped $CoS_2(001)$ is −0.12 eV, that of Pt-doped $CoS_2(001)$ is 0.03 eV, that of N-doped $CoS_2(001)$ is 0.07 eV, and that of O-doped $CoS_2(001)$ is −0.01 eV. Compared with that (0.25 eV) of the pure CoS_2 electrode, the $|\Delta G_{H^*}|$ of Ni-, Pt-, N-, and O-doped $CoS_2(001)$ electrode are much smaller when H is adsorbed at metal sites. It is noteworthy that $|\Delta G_{H^*}|$ of Pt-, N-, and O-doped $CoS_2(001)$ is smaller than that of Pt (0.08 eV), revealing their potential excellent electrochemical HER catalytic performance. And $|\Delta G_{H^*}|$ of O-doped $CoS_2(001)$ is closest to zero, which suggests that O-doped CoS_2 show the best HER catalytic activity among these doped CoS_2 material.

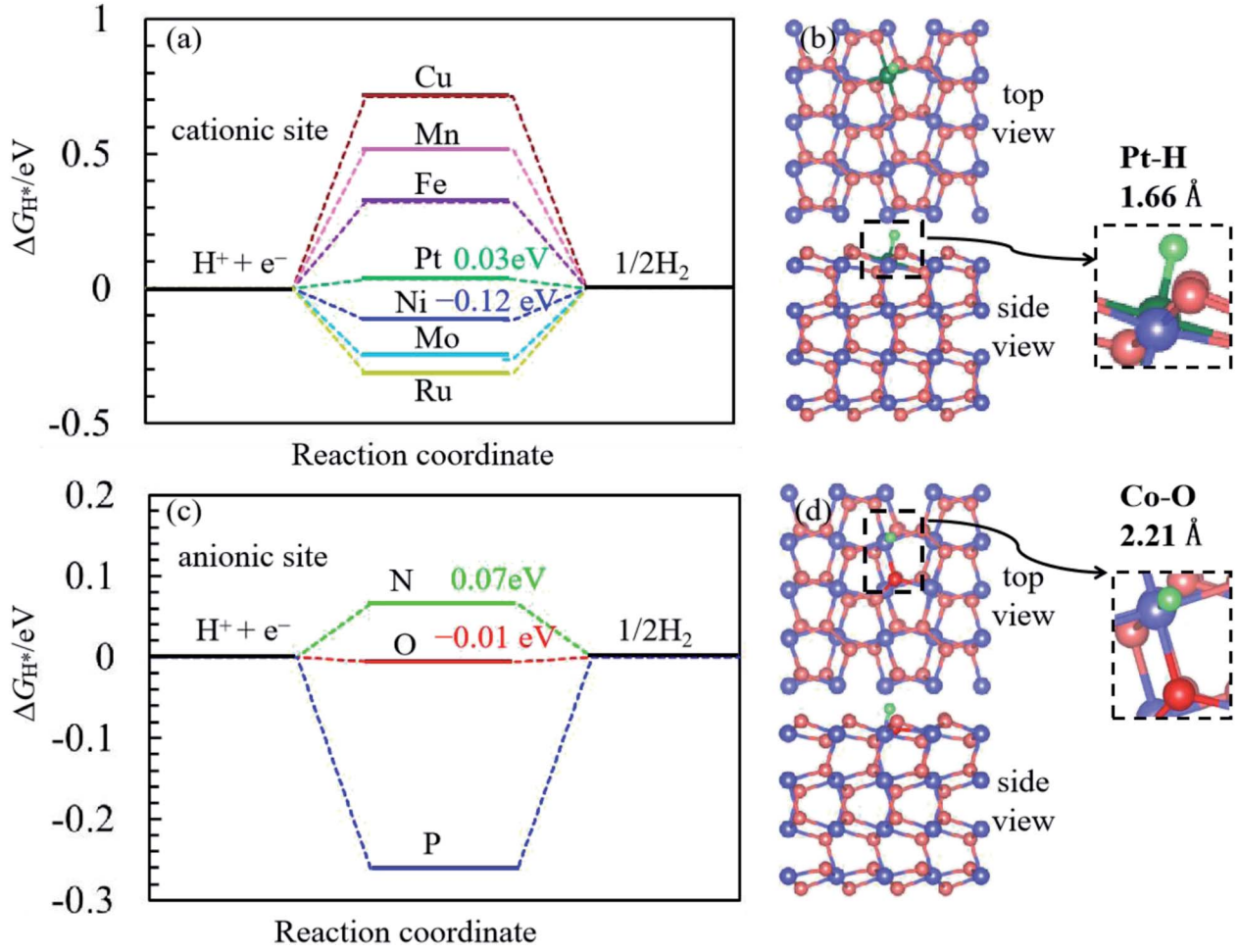

Fig. 4 (a) and (b) are ΔG_{H^*} diagram and the structure of Pt-doped $CoS_2(001)$ with H adsorption at Pt site, respectively. (c) and (d) are ΔG_{H^*} diagram and the structure of O-doped $CoS_2(001)$ with H adsorption at Co site, respectively. The blue, dark red, dark green, red balls and light green ball are Co, S, Pt, O and H atoms, respectively. Pt–H bond length is 1.66 Å and Co–O bond length is 2.21 Å.

Fig. 4(b) and (d) show the optimized structures of the Pt-doped CoS_2(001) with H adsorption at Pt site, Pt–H bond length is 1.66 Å, and that of the O-doped CoS_2(001) with H adsorption at Co site, Co–H bond length is 1.51 Å, respectively. To further explore why the electrochemical HER performance of CoS_2 at active metal sites *via* doping can be enhanced, the d-band centers of the active metal sites were calculated using the DFT method. We plotted in Fig. 5 the density of states for active metal sites used to H adsorption and marked the d-band center at active metal site with a dashed line. The d-band center of Co active site for the pristine CoS_2 is −2.06 eV and it is closest to the Fermi level. The d-band center of Cu active site for Cu-doped CoS_2 is −6.01 eV and it is farthest to the Fermi level. Meanwhile, ΔG_{H^*} for Cu-doped CoS_2 is 0.71 eV. To further probe the relationship between the d-band center of active metal site used to H adsorption and the Gibbs free energy of H adsorption on the active metal sites, a more detailed analysis diagram is plotted in Fig. 6. We can see from Fig. 6 that ΔG_{H^*} increases as the d-band centers of metal active sites decrease, which clearly illustrates that the binding between H adsorption atom and metal atom at the active site is weakened as the d band center is far away from the Fermi level. Our results just described are in line with investigations in the ΔG_{H^*} and d-band centers based on other materials.[26] This study reveals an intrinsic mechanism that d-band center of active metal site moves downwards after doping, leading to the weakening of hydrogen adsorption, which facilitates the desorption of H from the surface of CoS_2 as HER electrode material.

Based on our DFT calculations, we can find that Ni-, Pt-, O-, and N-doping can intrinsically promote the electrochemical HER catalytic performance of CoS_2 and a line in ΔG_{H^*} and d-band centers of H adsorption sites is achieved. The Pt-, O-, and N-doped CoS_2 show overpotentials of 0.03 V, 0.01 V, and 0.07 V, respectively, which are very close to values when using Pt, which is believed to be the best catalyst for the HER because

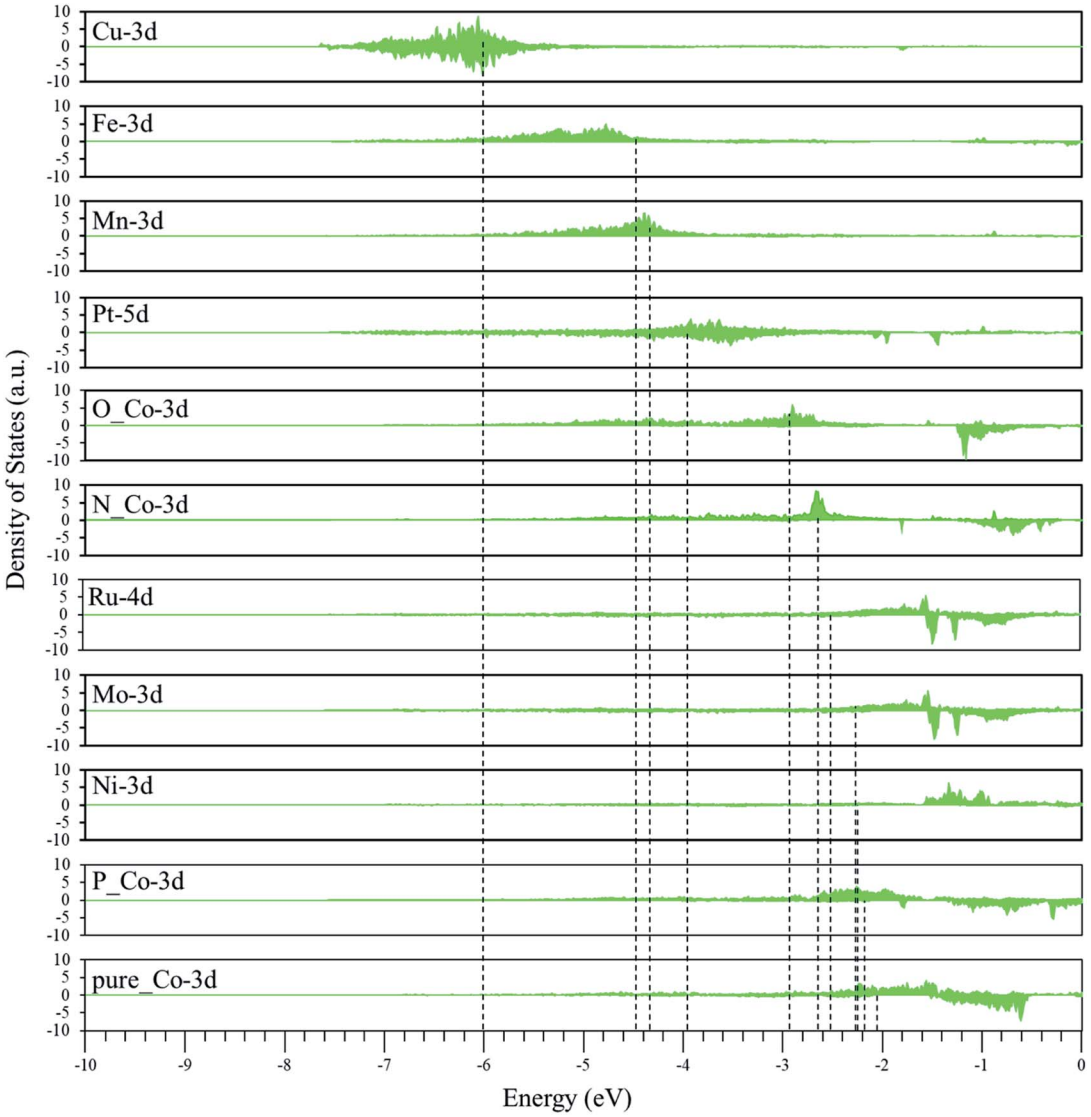

Fig. 5 The density of states at active metal sites. The dashed line marked the d-band center. The Fermi energy is set to zero.

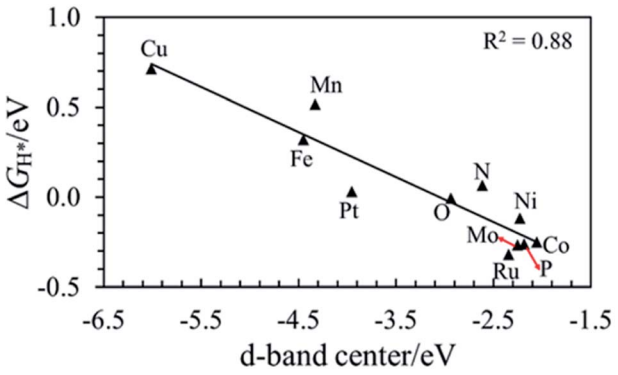

Fig. 6 The linear relationship between ΔG_{H^*} and d-band centers of H adsorption sites.

of its small overpotential (about 0.08 V).[3] Therefore, the CoS_2, after doping by Pt, O, and N becomes a promising catalyst.

4 Conclusions

In summary, we studied HER catalytic activities of cation/anion-doped CoS_2 as HER catalyst based on the DFT method. Our results reveal that the Pt-, N- and O-doped CoS_2 possesses an outstanding HER catalytic activity comparable to Pt. And a negative linear relationship was identified between ΔG_{H^*} and d-band centers of active metal sites. This exhibits that d-band center of active metal site moves downwards after cation/anion doping, leading to the weakening of hydrogen adsorption and facilitating the H desorption from the surface of CoS_2. Therefore, the intrinsic HER catalytic performance of CoS_2 can be improved by tailoring the d-band center of the active metal site. Based on this study, we can further explore the relationship between the structure and activity of CoS_2, which may shed light on the exploration of the potential use of other TMSs as HER electrode materials.

Conflicts of interest

There are no conflicts to declare.

Acknowledgements

This work is supported by the Fund Project of Chengdu Technological University under Grant No. 2020RC004.

References

1 Y. Tachibana, L. Vayssieres and J. R. Durrant, *Nat. Photonics*, 2012, **6**, 511–518.
2 B. Qiu, Y. Zhang, X. Guo, Y. Ma, M. Du, J. Fan, Y. Zhu, Z. Zeng and Y. Chai, *J. Mater. Chem. A*, 2022, **10**, 719–725.
3 J. K. Nørskov, T. Bligaard, A. Logadottir, J. R. Kitchin, J. G. Chen, S. Pandelov and U. Stimming, *ChemInform*, 2005, **152**, L5.
4 D. Saha, V. Patel, P. R. Selvaganapathy and P. Kruse, *Nanoscale Adv.*, 2022, **4**, 125–137.
5 B. Hinnemann, P. G. Moses, J. Bonde, K. P. Jørgensen, J. H. Nielsen, S. Horch, I. Chorkendorff and J. K. Nørskov, *J. Am. Chem. Soc.*, 2005, **127**, 5308–5309.
6 R. Li, J. Liang, T. Li, L. Yue, Q. Liu, Y. Luo, M. S. Hamdy, Y. Sun and X. Sun, *Chem. Commun.*, 2022, **15**, 633–644.
7 J. Tian, X. Xing, Y. Sun, X. Zhang, Z. Li, M. Yang and G. Zhang, *Chem. Commun.*, 2022, **58**, 557–560.
8 S. Mansingh, K. K. Das and K. Parida, *Sustainable Energy Fuels*, 2021, **5**, 1952–1987.
9 H. Wang, X. Xiao, S. Liu, C.-L. Chiang, X. Kuai, C.-K. Peng, Y.-C. Lin, X. Meng, J. Zhao, J. Choi, Y.-G. Lin, J.-M. Lee and L. Gao, *J. Am. Chem. Soc.*, 2019, **141**, 18578–18584.
10 J. Lee, J. Heo, H. Y. Lim, J. Seo, Y. Kim, J. Kim, U. Kim, Y. Choi, S. H. Kim, Y. J. Yoon, T. J. Shin, J. Kang, S. K. Kwak, J. Y. Kim and H. Park, *ACS Nano*, 2020, **14**, 17114–17124.
11 Y. Qu, H. Pan, C. Tat Kwok and Z. Wang, *Phys. Chem. Chem. Phys.*, 2015, **17**, 24820–24825.
12 Y. Lin, M. Yu, X. Li, W. Gao, L. Wang, X. Zhao, M. Zhou, X. Yao, M. He and X. Zhang, *J. Mater. Chem. C*, 2021, **9**, 15877–15885.
13 J. Xu, Y. Zhu, B. Yu, C. Fang and J. Zhang, *Inorg. Chem. Front.*, 2019, **6**, 3510–3517.
14 Z. Wang, K. Yu, R. Huang and Z. Zhu, *CrystEngComm*, 2021, **23**, 5097–5105.
15 N. Ran, B. Sun, W. Qiu, E. Song, T. Chen and J. Liu, *J. Phys. Chem. Lett.*, 2021, **12**, 2102–2111.
16 G. Chen, H. Li, Y. Zhou, C. Cai, K. Liu, J. Hu, H. Li, J. Fu and M. Liu, *Nanoscale*, 2021, **13**, 13604–13609.
17 Y. Dong, H. Sun and G. Liu, *Sustainable Energy Fuels*, 2021, **5**, 4115–4125.
18 Z. Shi, X. Qi, Z. Zhang, Y. Song, J. Zhang, C. Guo, W. Xu, K. Liu and Z. Zhu, *Nanoscale*, 2021, **13**, 6890–6901.
19 Y. Jiang, S. Gao, J. Liu, G. Xu, Q. Jia, F. Chen and X. Song, *Nanoscale*, 2020, **12**, 11573–11581.
20 Y. Zang, B. Yang, A. Li, C. Liao, G. Chen, M. Liu, X. Liu, R. Ma and N. Zhang, *ACS Appl. Mater. Interfaces*, 2021, **13**, 41573–41583.
21 C. n. Karakaya, N. Solati, U. Savacı, E. Keleş, S. Turan, S. Çelebi and S. Kaya, *ACS Catal.*, 2020, **10**, 15114–15122.
22 C. Karakaya, N. Solati, U. Savacı, E. Keleş, S. Turan, S. Çelebi and S. Kaya, *ACS Catal.*, 2020, **10**, 15114–15122.
23 J. Zhang, Y. Liu, B. Xia, C. Sun, Y. Liu, P. Liu and D. Gao, *Electrochim. Acta*, 2018, **259**, 955–961.
24 G. Papoian, J. K. Nørskov and R. Hoffmann, *J. Am. Chem. Soc.*, 2000, **122**, 4129–4144.
25 A. Vojvodic, A. Hellman, C. Ruberto and B. I. Lundqvist, *Phys. Rev. Lett.*, 2009, **103**, 146103.
26 Z. Chen, Y. Song, J. Cai, X. Zheng, D. Han, Y. Wu, Y. Zang, S. Niu, Y. Liu, J. Zhu, X. Liu and G. Wang, *Angew. Chem., Int. Ed.*, 2018, **57**, 5076–5080.
27 C. Tsai, K. Chan, J. K. Nørskov and F. Abild-Pedersen, *J. Phys. Chem. Lett.*, 2014, **5**, 3884–3889.
28 A. Maibam, S. Krishnamurty and M. Ahmad Dar, *Mater. Adv.*, 2022, **3**, 592–598.
29 A. Maibam, S. K. Das, P. P. Samal and S. Krishnamurty, *RSC Adv.*, 2021, **11**, 13348–13358.

30 J. M. Soler, E. Artacho, J. D. Gale, A. García, J. Junquera, P. Ordejón and D. Sánchez-Portal, *J. Phys.: Condens. Matter*, 2002, **14**, 2745–2779.
31 J. P. Perdew, K. Burke and M. Ernzerhof, *Phys. Rev. Lett.*, 1996, **77**, 3865–3868.
32 J. Zhang, Y. Liu, C. Sun, P. Xi, S. Peng, D. Gao and D. Xue, *ACS Energy Lett.*, 2018, **3**, 779–786.
33 J. Shi, Z. Wang and Y. Q. Fu, *J. Phys. D: Appl. Phys.*, 2016, **49**, 505601.
34 W. I. Choi, B. C. Wood, E. Schwegler and T. Ogitsu, *Adv. Energy Mater.*, 2015, **5**, 1501423.
35 J. K. Nørskov, T. Bligaard, J. Rossmeisl and C. H. Christensen, *Nat. Chem.*, 2009, **1**, 37–46.
36 D. Kim, J. Shi and Y. Liu, *J. Am. Chem. Soc.*, 2018, **140**, 9127–9131.
37 Q. Sun, Q. Wang, P. Jena and Y. Kawazoe, *J. Am. Chem. Soc.*, 2005, **127**, 14582–14583.
38 Y. Sun, A. Huang and Z. Wang, *RSC Adv.*, 2019, **9**, 26321–26326.
39 G. Feng, M. V. Ganduglia-Pirovano, C.-F. Huo and J. Sauer, *J. Phys. Chem. C*, 2018, **122**, 18445–18455.
40 A. Rasool, I. Anis, M. Dixit, A. Maibam, A. Hassan, S. Krishnamurty and M. A. Dar, *Catal. Sci. Technol.*, 2022, **12**, 310–319.